Porphyrin-Based Organoplatinum(II) Metallacycles With Enhanced Photooxidization Reactivity

Lintao Wu [1], Chun Han [1], Zhijun Wang [1], Xi Wu [1], Feng Su [1], Mengyao Li [1], Qingyang Zhang [2]* and Xiaobi Jing [3]*

[1] Department of Chemistry, Changzhi University, Changzhi, China, [2] State Key Laboratory of Bioactive Substances and Function of Natural Medicine, Institute of Materia Medica, Chinese Academy of Medical Sciences and Peking Union Medical College, Beijing, China, [3] School of Chemistry and Chemical Engineering, Yangzhou University, Yangzhou, China

In recent years, metal coordination macrocycles have obtained great interests due to the fact that they combined the rich host-guest properties of macro-cyclic hosts and the unique optical properties of the organic ligands. In this work, we constructed two porphyrin-based organoplatinum(II) metallacycles (**MC1** and **MC2**) through coordination-driven self-assembly. ^{1}H NMR, ^{31}P NMR, and HRMS technologies were used to characterize the structures of **MC1** and **MC2**. Interestingly, **MC1** and **MC2** can be used as catalysts for photooxidization under light irradiation with higher efficiency compared with the porphyrin ligand only. We hope that the coordination-driven self-assembly strategy can provide an efficient method to construct photo-active materials.

Keywords: self-assembly, macrocycle, porphyrin, photooxidization, coordination

INTRODUCTION

Macrocyclic host compounds, mainly including crown ethers (Zhu et al., 2012; Liu et al., 2017), cyclodextrins (Lai et al., 2017; Li et al., 2019), calixarenes (Kim et al., 2012; Nimse and Kim, 2013), cucurbiturils (Kim et al., 2007; Barrow et al., 2015), and pillararenes (Xue et al., 2012; Ogoshi et al., 2016; Yao et al., 2017; Chen J. et al., 2019), are the foundation of the development of supramolecular chemistry (Dong et al., 2014; Sun et al., 2018; Gao L. et al., 2019; Xiao et al., 2019). During the past two decades, the syntheses, host–guest properties, and applications of macrocycles have been widely investigated (Chen Y. et al., 2019; Wu and Yang, 2019). Among various macrocycles, discrete organoplatinum(II) metallacycles, which was fabricated by a new valuable strategy called "coordination-driven self-assembly," attracted great interests from both chemists and materials scientists (Gao S. et al., 2019; Zhang et al., 2019). A remarkable advantage of the "coordination-driven self-assembly" is that two-dimensional metallacycles or three-dimensional metallacages can be easily obtained by the formation of metal–ligand bonds between metal acceptors and organic donors when combining simple building blocks (Wang et al., 2019a; Yan et al., 2019). Up to now, discrete organoplatinum(II) metallacycles have been investigated a lot and widely applied in many areas, such as fluorescent detection, homogeneous catalysis, functional materials, bioengineering, photodynamic therapy, and so on (Cai et al., 2020; Qin et al., 2019).

Porphyrin derivatives, which contain a large π-conjugated aromatic structure, are a class of famous photo-activities (Liang et al., 2011; Ou et al., 2019; Wang et al., 2019b). Porphyrins usually have very intense absorption bands in the UV–visible region. However, due to the strong π-π stacking between the aromatic systems, porphyrins are easily aggregated in solvents, especially in aqueous solution (Zou et al., 2017). Commonly, porphyrins aggregate more seriously as

the concentration increased. This aggregation phenomenon greatly decreases the efficiency of porphyrins to generate $^1O_2$ and therefore restrained their potentially wide applications (Zhou et al., 2019). To address the aggregation of porphyrins in water, chemistry and materials scientists usually introduce a large substituent onto the platform of the porphyrin core (Slater et al., 2015). However, these chemical synthesis and purification processes have some other disadvantages, such as being time-consuming, tedious, and with higher costs of preparation.

Herein we designed and synthesized two new metallacycles (**MC1** and **MC2**) with *p*-bipyridine-modified porphyrin (**Scheme S1**, **Scheme 1**) as organic donor and organoplatinum(II) (**2** or **3**) as the metal acceptor (**Scheme 1**). The weak metal–ligand bonds will prevent the π-π stacking of the conjugated aromatic porphyrin units, thus improving the efficiency of generating $^1O_2$ under irradiation. Interestingly, compared with ligand **1** (**Figure S1**), the resultant metallacycle **MC1** or **MC2** can be used as catalyst for photo-oxidizing phenols much more efficiently.

MATERIALS AND METHODS
Synthesis of Metallacycles MC1 and MC2
Ligand **1** and organoplatinum(II) **2** (**Figure 1A**) and **3** (**Figure 1C**) were prepared according to a previous report (Grishagin et al., 2014). In a 1:1 molar ratio, bipyridylporphyrin **1** (1.85 mg, 3.00 μmol) and 60°Pt (II) acceptor **2** (4.01 mg, 3.00 μmol) were placed in a 2-ml vial, followed by addition of acetone (1 ml). After stirring overnight at 50°C, the mixture was filtered to remove insoluble materials (**Scheme S2**). Then, the solvent was removed by N_2 flow to about 0.2 ml, and **MC1** was obtained by the addition of diethyl ether (5.22 mg, 89%). **MC2** was prepared by the same method (**Scheme S3**).

MC1
Purple solid, 89%. ^{1}H NMR (400 MHz, CD$_3$COCD$_3$) δ (ppm): 10.17 (d, 4H), 9.21 (s, 2H), 8.92–8.90 (m, 10H), 8.27–8.25 (m, 8H), 7.89–7.85 (m, 12H), 2.47–2.43 (m, 24H), 1.70–1.62 (m, 36H). ^{31}P {^{1}H} NMR (acetone, room temperature, 121.4

MHz) δ = 9.53 (^{195}Pt satellites, $^1J_{Pt-P}$ = 2,662 Hz). HR-ESI-MS: calculated for $C_{203}H_{288}F_9N_{18}O_9P_{12}Pt_6S_3$ ([M – 3 OTf]$^{3+}$): 1,646.78, found: 1,646.77.

MC2
Purple solid, 87%. ^{1}H NMR (400 MHz, CD$_3$COCD$_3$) δ (ppm): 9.73 (s, 1H), 9.61 (s, 1H), 9.06 (s, 2H), 8.90 (s, 4H), 8.67–8.65 (m, 2H), 8.29–8.19 (m, 4H), 7.86–7.74 (m, 12H), 1.83–1.81 (m, 24H), 1.49–1.41 (m, 36H). ^{31}P {^{1}H} NMR (acetone, room temperature, 121.4 MHz) δ = −5.04 ppm (^{195}Pt satellites, $^1J_{Pt-P}$ = 3,156 Hz). HR-ESI-MS: calculated for $C_{244}H_{280}F_{12}N_{24}O_{20}P_8Pt_4S_4$ ([M + 8 CH$_3$COCH$_3$ – 4 OTf]$^{4+}$): 1,316.97, found: 1,316.92.

Materials
All reagents and solvents were commercially available in analytical grade and used as received. Further purification and drying by standard methods were employed and these were distilled prior to use when necessary. Deuterated solvents were purchased from Cambridge Isotope Laboratory (Andover, MA, USA). All evaporations of organic solvents were carried out with a rotary evaporator in conjunction with a water aspirator. Melting point measurements were taken on a hot-plate microscope apparatus and are uncorrected. ^{1}H and ^{13}C NMR spectra were recorded with an Aviance III 400 MHz or 600 MHz liquid-state NMR spectrometer. ^{31}P{^{1}H} NMR chemical shifts are referenced to an external unlocked sample of 85% H$_3$PO$_4$ (δ 0.0). Mass spectra were recorded on a Micromass Quattro II triple–quadrupole mass spectrometer using electrospray ionization with a MassLynx operating system. UV–vis spectra were recorded on a Hitachi F-7000 fluorescence spectrophotometer.
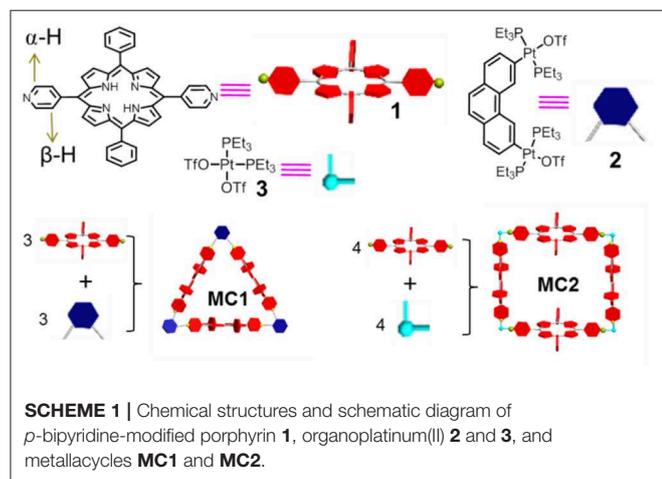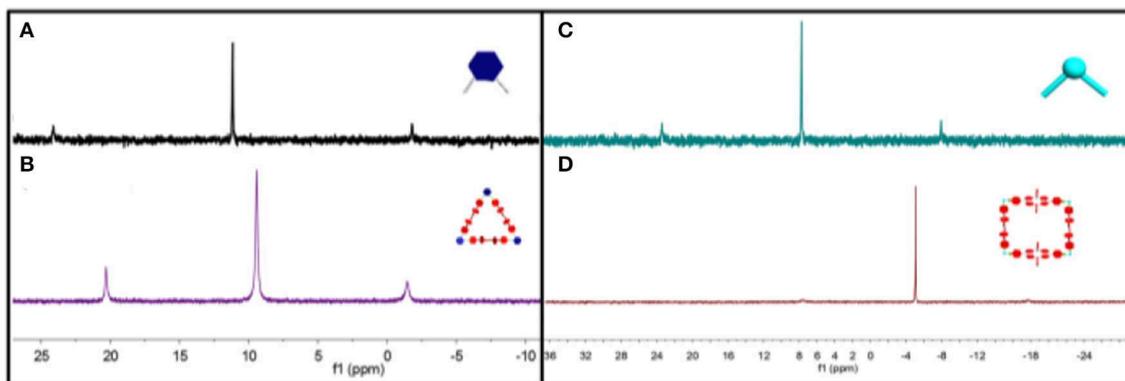
RESULTS AND DISCUSSION
NMR Studies
The formation of discrete organoplatinum(II) metallacycles **MC1** and **MC2** were characterized by multinuclear NMR (^{31}P and ^{1}H) analysis. The ^{31}P {^{1}H} NMR spectra of **MC1** and **MC2** showed a sharp singlet with concomitant ^{195}Pt satellites at 9.53 ppm for **MC1** and at −5.04 ppm for **MC2** (**Figures 1B,D**) corresponding to a single phosphorous environment, indicating the formation of discrete and symmetric metallacycles (Wei et al., 2014).

At the same time, downshifts were observed for β-pyridyl hydrogen in ^{1}H NMR spectra. As shown in **Figure 2**, β-pyridyl hydrogen changed from 9.04 to 9.51 and 9.72 ppm in **MC1** and from 9.04 to 10.21 ppm in **MC2**. β-pyridyl hydrogen also showed a downfield chemical shift. These chemical shift changes in ^{1}H NMR spectra are similar with the previous analogous organoplatinum(II) system, indicating the formation of discrete metallacycles (Yao et al., 2018).

Electrospray Ionization Time of Flight Mass Spectrometry Studies
Electrospray ionization time of flight mass spectrometry (ESI-TOF-MS) provided further evidence for the stoichiometry formation of discrete metallacycles **MC1** and **MC2**. In the mass spectrum of **MC1**, the peak at m/z = 1,646.77 is consistent with

SCHEME 1 | Chemical structures and schematic diagram of *p*-bipyridine-modified porphyrin **1**, organoplatinum(II) **2** and **3**, and metallacycles **MC1** and **MC2**.

FIGURE 1 | ^{31}P{^{1}H} NMR spectra (room temperature, 121.4 MHz) of **(A)** 60° acceptor **2**, **(B)** metallacycle **MC1**, **(C)** 90° acceptor **3**, and **(D)** metallacycle **MC2** in acetone.
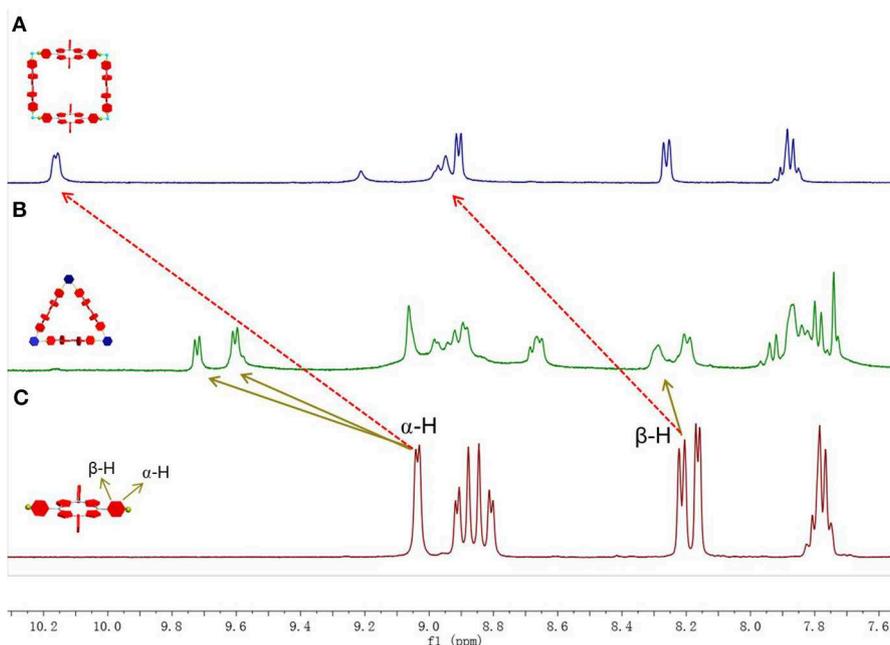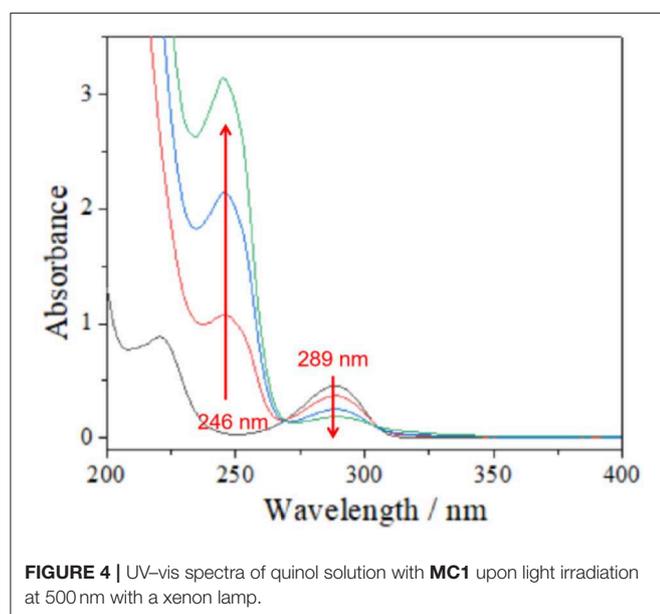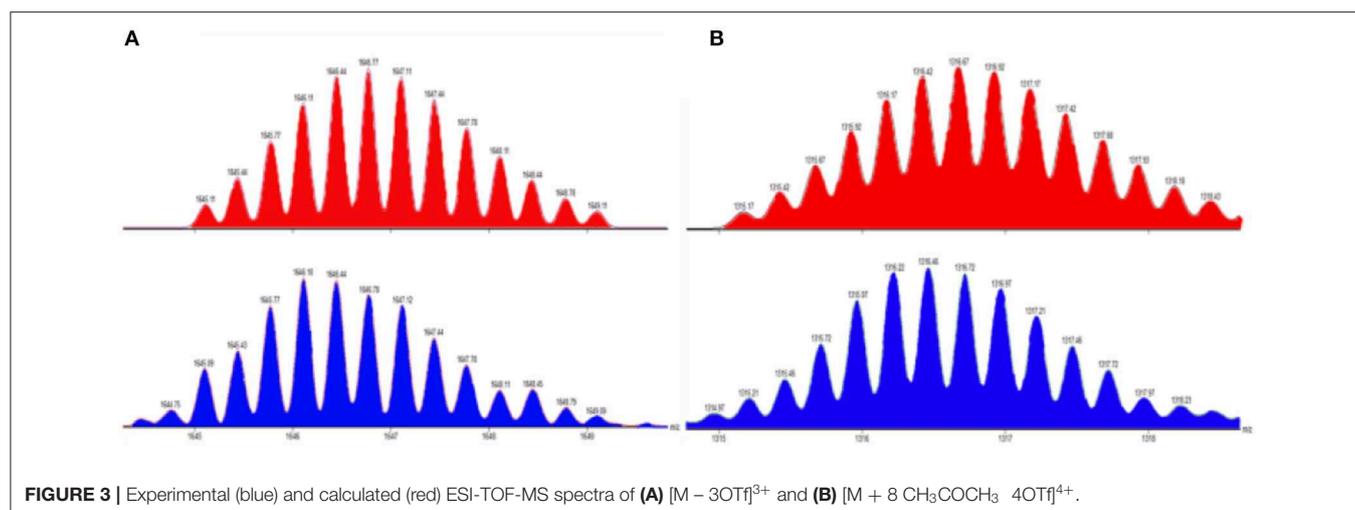

FIGURE 2 | ^{1}H NMR spectra (CD$_3$COCD$_3$, room temperature) of **(A)** bipyridylporphyrin **1**, **(B)** metallacycle **MC1**, and **(C)** metallacycle **MC2**.

an intact [M – 3OTf]$^{3+}$ charge state, which supported a [3 + 3] metallacycle (**Figure 3A**). Similarly, for metallacycle **MC2**, the peak at m/z = 1,316.92 is consistent with an intact [M + 8 CH$_3$COCH$_3$ $^-$ 4OTf]$^{4+}$ charge state, which is expected only for a [4 + 4] metallacycle (**Figure 3B**). All the evidence from ^{1}H NMR, ^{31}P NMR, and ESI-TOF-MS confirmed the formation of a discrete structure as the sole assembly product.

Photooxidization Studies

As we all know, porphyrins have the ability to generate ^{1}O$_2$ due to the fact that they could be excited into ^{3}O$_2$ state under irradiation and the energy transfer process is accompanied with molecular O$_2$. However, due to the strong π-π interactions,

most porphyrins applied as photosensitizers are easily aggregated in aqueous solution (**Figures S4**, **S5**). This aggregation will greatly restrain the ability of the porphyrins to generate reactive oxygen species. For our obtained metallacycles **MC1** and **MC2**, the coordination bonds will decrease the self-quenching of the excited states and improve the photooxidization efficiency. Therefore, metallacycles **MC1** and **MC2** can be used as an expected catalyst for the photoreaction mediated by ^{1}O$_2$. Herein quinol was selected as a model substrate for detecting the reactivity, and UV–vis spectroscopy was used to monitor the process. As shown in **Figure 4**, after 20 ml of aqueous solution of quinol (10^{-2} mmol L^{-1}) was irradiated by a LED lamp (500 nm) under air with **MC1** (5 mg) as catalyst, the absorption band

FIGURE 3 | Experimental (blue) and calculated (red) ESI-TOF-MS spectra of **(A)** $[M - 3OTf]^{3+}$ and **(B)** $[M + 8\ CH_3COCH_3\ 4OTf]^{4+}$.

FIGURE 4 | UV–vis spectra of quinol solution with **MC1** upon light irradiation at 500 nm with a xenon lamp.

metallacycles were characterized by ^{31}P NMR, ^{1}H NMR, and ESI-TOF-MS methods. Furthermore, the metallacycles **MC1** and **MC2** can be used as an expected catalyst for the photoreaction mediated by $^{1}O_2$ due to the coordination bonds that will decrease the self-quenching of the excited states of porphyrin units and improve the photooxidization efficiency. Our next study will focus on the application of our metallacycles in photodynamic therapy.

DATA AVAILABILITY STATEMENT

All datasets generated for this study are included in the article/**Supplementary Material**.

AUTHOR CONTRIBUTIONS

LW, CH, and ZW prepared the ligands. LW, XW, and FS constructed the metallacycles. ML and QZ did the photooxidization. LW and XJ analyzed the data. LW, QZ, and XJ wrote the paper.

FUNDING

of the phenyl moiety in quinol in 289 nm gradually decreased, and 65% of quinol was consumed after irradiation for 60 min (**Figure 4**). As expected, **MC2** has a similar catalytic efficiency with **MC1** (**Figure S2**). However, in the control experiments using the ligand **1** as catalyst instead of **MC1**, only 8% of quinol was reacted after irradiation at 500 for 60 min under the same conditions (**Figure S2**). Importantly, the investigation for the recyclability of **MC1** showed that they could be recovered by simple filtration and reused without significant loss of catalytic activity (yield loss within 5% for six cycles, **Figure S3**).

CONCLUSIONS

In this paper, we synthesized two metallacycles, **MC1** and **MC2**, with *p*-bipyridines modified porphyrin as the ligands through coordination-driven self-assembly. Then, the obtained

SUPPLEMENTARY MATERIAL

The Supplementary Material for this article can be found online at: https://www.frontiersin.org/articles/10.3389/fchem.2020.00262/full#supplementary-material

REFERENCES

Barrow, S. J., Kasera, S., Rowland, M. J., Barrio, J., and Scherman, O. A. (2015). Cucurbituril-based molecular recognition. *Chem. Rev.* 115:12320. doi: 10.1021/acs.chemrev.5b00341

Cai, Y., Wang, Y., Wang, C., Long, R., Cao, L., Chen, Y., et al. (2020). Hierarchical self-assembly of 3D amphiphilic discrete organoplatinum(II) metallacage in water. *Chin. Chem. Lett.* 31, 689–692. doi: 10.1016/j.cclet.2019.08.036

Chen, J., Wang, Y., Wang, C., Long, R., Chen, T., and Yao, Y. (2019). Functionalization of inorganic nanomaterials with pillar[n]arenes. *Chem. Commun.* 55, 6817–6826. doi: 10.1039/C9CC03165K

Chen, Y., Sun, S., Lu, D., Shi, Y., and Yao, Y. (2019). Water-soluble supramolecular polymers constructed by macrocycle-based host-guest interactions. *Chin. Chem. Lett.* 30, 37–43. doi: 10.1016/j.cclet.2018.10.022

Dong, S., Zheng, B., Wang, F., and Huang, F. (2014). Supramolecular polymers constructed from macrocycle-based host–guest molecular recognition motifs. *Acc. Chem. Res.* 47, 1982–1994. doi: 10.1021/ar5000456

Gao, L., Li, M., Ehrmann, S., Tu, Z., and Haag, R. (2019). Positively charged nanoaggregates based on zwitterionic pillar[5]arene that combat planktonic bacteria and disrupt biofilms. *Angew. Chem. Int. Ed.* 58, 3645–3649. doi: 10.1002/anie.201810314

Gao, S., Yan, X., Xie, G., Zhu, M., Ju, X., Stang, P. J., et al. (2019). Membrane intercalation-enhanced photodynamic inactivation of bacteria by a metallacycle and TAT-decorated virus coat protein. *Proc. Natl. Acad. Sci. U.S.A.* 116, 23437–23443. doi: 10.1073/pnas.1911869116

Grishagin, I. V., Pollock, J. B., Kushal, S., Cook, T. R., Stang, P. J., and Olenyuk, B. Z. (2014). *In vivo* anticancer activity of rhomboidal Pt(II) metallacycles. *Proc. Natl. Acad. Sci. U.S.A.* 111, 18448–18453. doi: 10.1073/pnas.1418712111

Kim, H. J., Lee, M. H., Mutihac, L., Vicens, J., and Kim, J. S. (2012). Host–guest sensing by calixarenes on the surfaces. *Chem. Soc. Rev.* 41, 1173–1190. doi: 10.1039/C1CS15169J

Kim, K., Selvapalam, N., Ko, Y. H., Park, K. M., Kim, D., and Kim, J. (2007). Functionalized cucurbiturils and their applications. *Chem. Soc. Rev.* 36, 267–279. doi: 10.1039/B603088M

Lai, W.-F., Rogach, A. L., and Wong, W.-T. (2017). Chemistry and engineering of cyclodextrins for molecular imaging. *Chem. Soc. Rev.* 46, 6379–6419. doi: 10.1039/C7CS00040E

Li, P.-Y., Chen, Y., Chen, C.-H., and Liu, Y. (2019). Amphiphilic multi-charged cyclodextrins and vitamin K co-assembly as a synergistic coagulant. *Chem. Commun.* 55:11790. doi: 10.1039/C9CC06545H

Liang, X., Li, X., Yue, X., and Dai, Z. (2011). Conjugation of porphyrin to nanohybrid cerasomes for photodynamic diagnosis and therapy of cancer. *Angew. Chem. Int. Ed.* 50, 11622–11627. doi: 10.1002/anie.2011 03557

Liu, Z., Nalluri, S. K. M., and Stoddart, J. F. (2017). Surveying macrocyclic chemistry: from flexible crown ethers to rigid cyclophanes. *Chem. Soc. Rev.* 46, 2459–2478. doi: 10.1039/C7CS00185A

Nimse, S. B., and Kim, T. (2013). Biological applications of functionalized calixarenes. *Chem. Soc. Rev.* 42, 366–386. doi: 10.1039/C2CS3 5233H

Ogoshi, T., Yamagishi, T.-,a., and Nakamoto, Y. (2016). Pillar-shaped macrocyclic hosts pillar[n]arenes: new key players for supramolecular chemistry. *Chem. Rev.* 116, 7937–8002. doi: 10.1021/acs.chemrev.5b00765

Ou, C., Zhang, Y., Pan, D., Ding, K., Zhang, S., Xu, W., et al. (2019). Zinc Porphyrin-polydopamine core-shell nanostructures for enhanced photodynamic/photothermal cancer therapy. *Mater. Chem. Front.* 3, 1786–1792. doi: 10.1039/C9QM00197B

Qin, Y., Chen, L.-J., Dong, F., Jiang, S.-T., Yin, G.-Q., Li, X., et al. (2019). Light-controlled generation of singlet oxygen within a discrete dual-stage metallacycle for cancer therapy. *J. Am. Chem. Soc.* 141, 8943–8950. doi: 10.1021/jacs.9b02726

Slater, A. G., Hu, Y., Yang, L., Argent, S. P., Lewis, W., Blunt, M. O., et al. (2015). Thymine functionalised porphyrins, synthesis and heteromolecular surface-based self-assembly. *Chem. Sci.* 5, 1562–1569. doi: 10.1039/C4SC0 3531C

Sun, S., Geng, M., Huang, L., Chen, Y., Cen, M., Lu, D., et al. (2018). A new amphiphilic pillar[5]arene: synthesis and controllable self-assembly in water and application in white-light-emitting systems. *Chem. Commun.* 54, 13006–13009. doi: 10.1039/C8CC07658H

Wang, Y., Cai, Y., Cao, L., Cen, M., Chen, Y., Zhang, R., et al. (2019a). An amphiphilic metallaclip with enhanced fluorescence emission in water: synthesis and controllable self-assembly into multi-dimensional micro-structures. *Chem. Commun.* 55, 10132–10134. doi: 10.1039/C9CC04809J

Wang, Y., Wang, C., Long, R., Cao, Y., Fan, D., Cen, M., et al. (2019b). Synthesis and controllable self-assembly of 3D amphiphilic organoplatinum(II) metallacages in water. *Chem. Commun.* 55, 5167–5170. doi: 10.1039/C9CC02173F

Wei, P., Cook, T. R., Yan, X., Huang, F., and Stang, P. J. (2014). A discrete amphiphilic organoplatinum(II) metallacycle with tunable lower critical solution temperature behavior. *J. Am. Chem. Soc.* 136, 15497–15500. doi: 10.1021/ja5093503

Wu, J.-R., and Yang, Y.-W. (2019). New opportunities in synthetic macrocyclic arenes. *Chem. Commun.* 55, 1533–1543. doi: 10.1039/C8CC09374A

Xiao, T., Zhou, L., Xu, L., Zhong, W., Zhao, W., Sun, X.-Q., et al. (2019). Dynamic materials fabricated from water soluble pillar[n]arenes bearing triethylene oxide groups. *Chin. Chem. Lett.* 30, 271–276. doi: 10.1016/j.cclet.2018.05.039

Xue, M., Yang, Y., Chi, C., Zhang, Z., and Huang, F. (2012). Pillararenes, a new class of macrocycles for supramolecular chemistry. *Acc. Chem. Res.* 45, 1294–1308. doi: 10.1021/ar2003418

Yan, X., Wei, P., Liu, Y., Wang, M., Chen, C., Zhao, J., et al. (2019). Endo- and exo-functionalized tetraphenylethylene M12L24 nanospheres: fluorescence emission inside a confined space. *J. Am. Chem. Soc.* 141, 9673–9679. doi: 10.1021/jacs.9b03885

Yao, Y., Sun, Y., Yu, H., Chen, W., Dai, H., and Shi, Y. (2017). A pillar[5]arene based gel from a low-molecular-weight gelator for sustained dye release in water. *Dalton Trans.* 46, 16802–16806. doi: 10.1039/C7DT04001F

Yao, Y., Zhao, R., Shi, Y., Cai, Y., Chen, J., Sun, S., et al. (2018). 2D amphiphilic organoplatinum(II) metallacycles: their syntheses, self-assembly in water and potential application in photodynamic therapy. *Chem. Commun.* 54, 8068–8071. doi: 10.1039/C8CC04423F

Zhang, Z., Zhao, Z., Hou, Y., Wang, H., Li, X., He, G., et al. (2019). Aqueous platinum(II) cage-based light-harvesting system for photocatalytic cross-coupling hydrogen evolution reaction. *Angew. Chem. Int. Ed.* 58, 8862–8866. doi: 10.1002/anie.201904407

Zhou, W.-L., Zhao, X., Chen, Y., and Liu, Y. (2019). Construction and heterogeneous photooxidization reactivity of a cyclodextrin/porphyrin polyrotaxane network. *Org. Chem. Front.* 6, 10–14. doi: 10.1039/C8QO00790J

Zhu, K., Vukotic, V. N., Noujeim, N., and Loeb, S. J. (2012). Bis(benzimidazolium) axles and crown ether wheels: a versatile templating pair for the formation of [2]rotaxane molecular shuttles. *Chem. Sci.* 3, 3265–3271. doi: 10.1039/c2sc20986a

Zou, Q., Abbas, M., Zhao, L., Li, S., Shen, G., and Yan, X. (2017). Biological photothermal nanodots based on self-assembly of peptide–porphyrin conjugates for antitumor therapy. *J. Am. Chem. Soc.* 139, 1921–1927. doi: 10.1021/jacs.6b11382